Acta Crystallographica Section B
Structural Science
ISSN 0108-7681

New electron diffraction method to identify the chirality of enantiomorphic crystals

Haruyuki Inui, Akihiro Fujii, Katsushi Tanaka, Hiroki Sakamoto and Kazuo Ishizuka

Acta Crystallographica Section B
Structural Science
ISSN 0108-7681

New electron diffraction method to identify the chirality of enantiomorphic crystals

Haruyuki Inui,[a]* Akihiro Fujii,[a] Katsushi Tanaka,[b] Hiroki Sakamoto[a] and Kazuo Ishizuka[c]

[a]Department of Materials Science and Engineering, Kyoto University, Sakyo-ku, Kyoto 606-8501, Japan, [b]Department of Advanced Materials Science, Kagawa University, 2217-20 Hayashi-cho, Takamatsu, Kagawa 761-0396, Japan, and [c]HREM Research Inc., 14-48 Matsukazedai, Higashimatsuyama, Saitama 355-0055, Japan

Correspondence e-mail: inui@mtl.kyoto-u.ac.jp

Received 24 September 2003
Accepted 20 October 2003

A new CBED (convergent-beam electron diffraction) method is proposed for the identification of the chirality of enantiomorphic crystals, in which asymmetry in the intensity of the reflections of Bijvoet pairs in an experimental symmetrical zone-axis CBED pattern is compared with that of a computer-simulated CBED pattern. The intensity difference for reflections of these Bijvoet pairs results from multiple scattering (dynamical nature of electron diffraction) among relevant Bijvoet pairs of reflections, each pair of which has identical amplitude and different phase angles. Therefore, the crystal thickness where chiral identification is made with the present method is limited by the extinction distance of Bijvoet pairs of reflections relevant to multiple scattering to produce the intensity asymmetry, which is usually of the order of a few tens of nanometers. With the present method, a single CBED pattern is sufficient and chiral identification can be made for all the possible enantiomorphic crystals that are allowed to exist in crystallography.

1. Introduction

Enantiomorphism is usually referred to and used to describe objects that are lacking in improper rotations (rotoinversions and rotoreflections). Owing to the absence of a center of symmetry ($\overline{1}$), a mirror plane ($m = \overline{2}$) and a $\overline{4}$ axis, such enantiomorphic (chiral) crystals or molecules can occur in two different forms that are related as a right hand to a left hand and these enantiomorphically related crystals belong to any of the 11 crystal classes (point groups), as summarized in Table 1 (Mead, 1974; Burns & Glazer, 1990; Hahn, 1996). In general, the right-handed crystal can be converted to the left-handed one by changing the coordinates of the atom positions from (x, y, z) to $(-x, -y, -z)$. For enantiomorphic crystals that are related to each other by a screw axis (known as an enantiomorphic space-group pair), a change in space-group number is needed in addition to the atomic coordinate conversion (Hahn, 1996). These crystals are mirror-related and are not superimposable with each other. One of the two enantiomorphic crystals exhibits optical bioactivities which are different from the other crystal in most cases (Mason, 1982; Crossley, 1995; Brown, 1997). Therefore, the distinction of the chirality of enantiomorphic crystals is sometimes very important, as in the well known example of the Thalidomide accident, which occurred as a tragedy owing to the harmful side effects of one of the two enantiomorphic crystals. The distinction of chirality in enantiomorphic crystals is usually made by X-ray diffraction (Glusker & Trueblood, 1972; James, 1982; Stout & Jensen, 1989; Glusker *et al.*, 1994). Friedel's law states that members of a Friedel pair, which are Bragg

Table 1
Crystal system, crystal class (point group), the equivalent indices of Bijvoet pairs of reflections in the asymmetric unit and the appropriate zone-axis orientations for the chiral identification of crystals belonging to all the possible enantiomorphic point groups.

The nomenclature 'ZOLZ' in the last column indicates the Bijvoet pairs of reflections that appear in ZOLZ as $\pm\mathbf{g}$ are utilized for chiral identification.

		Bijvoet pairs		
Crystal system	Point group	Equivalent indices	Equivalent indices	Appropriate zone-axis
Triclinic	1	hkl	$\overline{h}\overline{k}\overline{l}$	*ZOLZ*
Monoclinic	2	$hkl = \overline{h}k\overline{l}$	$\overline{h}\overline{k}l = h\overline{k}l$	$\langle h0l\rangle$
Orthorhombic	222	$hkl = h\overline{k}\overline{l} = \overline{h}k\overline{l} = \overline{h}\overline{k}l$	$\overline{h}\overline{k}\overline{l} = \overline{h}kl = h\overline{k}l = hk\overline{l}$	$\langle hk0\rangle$, $\langle 0kl\rangle$, $\langle h0l\rangle$
Tetragonal	4	$hkl = \overline{k}hl = \overline{h}\overline{k}l = k\overline{h}l$	$\overline{h}\overline{k}l = k\overline{h}l = hk\overline{l} = \overline{k}h\overline{l}$	$\langle hk0\rangle$
	422	$hkl = \overline{k}hl = \overline{h}\overline{k}l = k\overline{h}l = h\overline{k}\overline{l} = \overline{k}\overline{h}\overline{l} = \overline{h}k\overline{l} = kh\overline{l}$	$\overline{h}\overline{k}l = k\overline{h}l = hk\overline{l} = \overline{k}h\overline{l} = \overline{h}kl = khl = h\overline{k}\overline{l} = \overline{k}\overline{h}l$	$\langle hk0\rangle$, $\langle h0l\rangle$, $\langle hhl\rangle$
Trigonal	3	$hkil$	$\overline{h}\overline{k}\overline{i}\overline{l}$	*ZOLZ*
	32†			
	321	$hkil = hik\overline{l}$	$\overline{h}\overline{k}\overline{i}l = \overline{h}\overline{i}kl$	$\langle h\overline{h}0l\rangle$
	312	$hkil = \overline{h}\overline{i}kl$	$\overline{h}\overline{k}\overline{i}l = hikl$	$\langle hh\overline{2}hl\rangle$
Hexagonal	6	$hkil = \overline{h}\overline{k}il$	$\overline{h}\overline{k}\overline{i}l = hki\overline{l}$	$\langle hki0\rangle$
	622	$hkil = \overline{h}\overline{k}il = hik\overline{l} = \overline{h}\overline{i}k\overline{l}$	$\overline{h}\overline{k}\overline{i}l = hki\overline{l} = \overline{h}\overline{i}kl = hikl$	$\langle h\overline{h}0l\rangle$, $\langle hh\overline{2}hl\rangle$, $\langle hki0\rangle$
Cubic	23	$hkl = h\overline{k}\overline{l} = \overline{h}k\overline{l} = \overline{h}\overline{k}l$	$\overline{h}\overline{k}l = \overline{h}kl = h\overline{k}l = hk\overline{l}$	$\langle hk0\rangle$
	432	$hkl = h\overline{k}\overline{l} = \overline{h}k\overline{l} = \overline{h}\overline{k}l = \overline{h}lk = h\overline{l}k = hl\overline{k} = \overline{h}\overline{l}\overline{k}$	$\overline{h}\overline{k}l = \overline{h}kl = h\overline{k}l = hk\overline{l} = h\overline{l}\overline{k} = \overline{h}l\overline{k} = \overline{h}lk = hlk$	$\langle hk0\rangle$, $\langle hhl\rangle$

† The point group 32 in the rhombohedral coordinate system is divided into two space groups, 321 and 312 in the hexagonal coordinate system.

reflections related to each other by inversion through the origin, have equal amplitude ($|F|$) and opposite phase (φ), as shown below (Ramaseshan, 1964; Srinivasan, 1972)

$$\left|F(hkl)\right| = \left|F(\overline{h}\overline{k}\overline{l})\right| \text{ and } \varphi(hkl) = -\varphi(\overline{h}\overline{k}\overline{l}), \qquad (1)$$

where F and hkl represent the structure factors and the index of reflection, respectively. In X-ray diffraction, the breakdown of Friedel's law occurs through anomalous scattering, resulting in different intensities and phase angles for the Friedel pair of reflections (Ramaseshan, 1964; Srinivasan, 1972). Bijvoet pairs are Bragg reflections which are space-group symmetry equivalents to the two members of a Friedel pair and they are usually used in the identification of the chirality of a crystal rather than the Friedel pairs through the inspection of the intensity asymmetry between the pairs (Bijvoet *et al.*, 1951), as the Bijvoet relation states as follows

$$F_R(hkl) = F_L(\overline{h}\overline{k}\overline{l}) \text{ and } F_R(\overline{h}\overline{k}\overline{l}) = F_L(hkl), \qquad (2)$$

where the subscripts R and L represent right- and left-handed crystals, respectively. However, distinction of chirality by X-ray diffraction usually needs a relatively large-sized single crystal of high quality that is free from crystal lattice defects (McPherson, 1982; Drenth, 1994). In addition, special techniques, such as the multiple isomorphous replacement (MIR) method, and a sufficiently strong X-ray beam, such as that from a synchrotron radiation source, are needed in many cases (Drenth, 1994).

If the distinction can be made by electron diffraction in the transmission electron microscope (TEM), such difficulties can be completely avoided owing to the capability of the TEM of using a nanometer-sized electron probe (Reimer, 1984; Spence & Zuo, 1992; Williams & Carter, 1996). However, it is generally believed that electron diffraction is not a general method for the chiral identification of enantiomorphic crystals since the intensity difference is not expected to occur for Bijvoet pairs of reflections through anomalous scattering, which does not occur in electron diffraction (Cowley, 1986). Thus, Bijvoet pairs of reflections have long been ignored by transmission electron microscopists. Although a few methods have so far been proposed to determine the chirality of enantiomorphic crystals such as quartz (Goodman & Secomb, 1977; Goodman & Johnson, 1977) and MnSi (Tanaka *et al.*, 1985) by electron diffraction, in particular by the convergent-beam electron diffraction (CBED) method (Spence & Zuo, 1992, Tanaka & Terauchi, 1985), none of them can be easily extended to other enantiomorphic crystals (see Table 1 for the point groups of possible enantiomorphic crystals). Here we show, however, that the intensity difference can indeed be observed for Bijvoet pairs even in electron diffraction because of its dynamical nature (multiple scattering), once an appropriate zone-axis orientation is chosen so that Bijvoet pairs of reflections are arranged

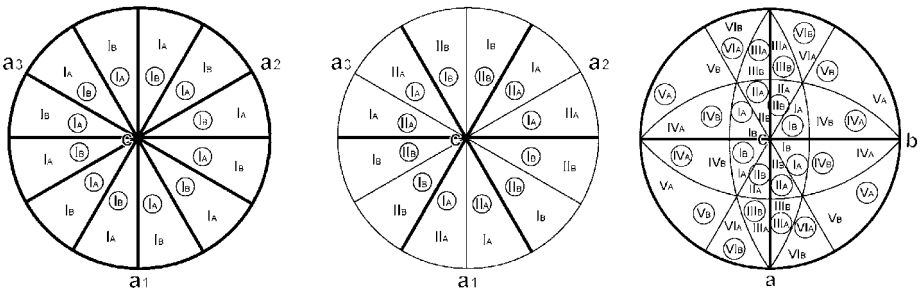

(*a*) 622 (*b*) 321 (*c*) 222

Figure 1
Distribution of the Bijvoet pairs of reflections located in the standard triangles for point groups (*a*) 622, (*b*) 321 and (*c*) 222. Bijvoet pairs of reflections are expressed as I_A–I_B, II_A–II_B *etc.* and the symbols expressed with ○ indicate reflections that appear on the reverse side of the triangles.

symmetrically in a zone-axis CBED pattern. Then, the chiral identification is made by noting the intensity asymmetry between Bijvoet pairs of reflections. The proposed method can be easily extended to identify the chirality of all crystallographically possible enantiomorphic crystals.

2. Appropriate zone-axis orientations that enable the symmetrical observation of Bijvoet pairs of reflections

One of the most important requirements of this new method is the choice of an appropriate zone-axis orientation (incident beam direction) so that Bijvoet pairs of reflections appear symmetrically in a single CBED pattern. For this purpose, any reflections belonging to the ZOLZ (zeroth-order Laue zone) or FOLZ (first-order Laue zone) can be used. Since the *hkl* reflections that correspond to Bijvoet pairs depend on the point group (Table 1), the appropriate symmetrical zone-axis orientations depend on the point group of the crystal. Appropriate zone-axis orientations can thus be found by plotting the distribution of the Bijvoet pairs for a particular type of *hkl* reflection located in the standard triangles in the stereographic projection. The particular type of *hkl* reflection denotes, for example, twelve $12\bar{3}4$-type reflections for a crystal with hexagonal symmetry. Since Bijvoet pairs, for example, for crystals with the point group 622 are

$$hkil = \overline{hki}l = hik\bar{l} = \overline{hik}l \text{ and } \overline{hkil} = hki\bar{l} = \overline{hik}l = hikl,$$

Bijvoet pairs (expressed as I_A and I_B) for a particular type of reflection distribute in the stereographic projection as shown in Fig. 1(*a*). Then, the appropriate zone-axis orientations at which the Bijvoet pairs of reflection disks appear symmetrical in a single CBED pattern are readily known as those on $\langle 11\bar{2}0\rangle$, $\langle 1\bar{1}00\rangle$ and [0001] zone circles, as illustrated in Fig. 1(*a*). Therefore, the appropriate zone-axis orientations in this case are $\langle h\bar{h}0l\rangle$, $\langle hh\bar{2}hl\rangle$ and $\langle hki0\rangle$. For crystals with point groups 32 and 222, there are two and six, respectively, different types of Bijvoet pairs for a particular type of reflection, as illustrated with I_A–I_B, II_A–II_B and so on in Figs. 1(*b*) and (*c*), respectively. Stereographic analysis indicates that the appropriate zone-axis orientations in these cases are of the $\langle h\bar{h}0l\rangle$-type and of the $\langle hk0\rangle$-, $\langle 0kl\rangle$- and $\langle h0l\rangle$-types, respectively. Similarly, the appropriate zone-axis orientations are determined in Table 1 (the fifth column) for all the point groups that have a pair of enantiomorphic crystals. As seen in Table 1, nine of the 11 point groups that have enantiomorphic crystals have the appropriate zone-axis orientations in which Bijvoet pairs of reflections appear symmetrically in a single CBED pattern. The method of chiral identification for crystals belonging to these nine point groups will be described in §3. The other two point groups, 1 and 3, in which each of the two members of a Bijvoet pair of reflections do not have any equivalent reflections, do not have the appropriate zone-axis orientations to observe Bijvoet pairs of reflections symmetrically. However, since Bijvoet pairs of reflections appear in ZOLZ as opposite reflections ($\pm\mathbf{g}$; $\mathbf{g}$ denotes a reflection vector) with respect to the transmitted (center) beam, chiral identification is possible even in these two cases by observing the asymmetry of the intensity for these ZOLZ reflections of opposite sign, as will be described in §4. The nomenclature 'ZOLZ' in Table 1 for these two point groups therefore means that Bijvoet pairs of reflections that appear in ZOLZ as $\pm\mathbf{g}$ reflections are utilized for chiral identification without specifying the zone-axis orientations.

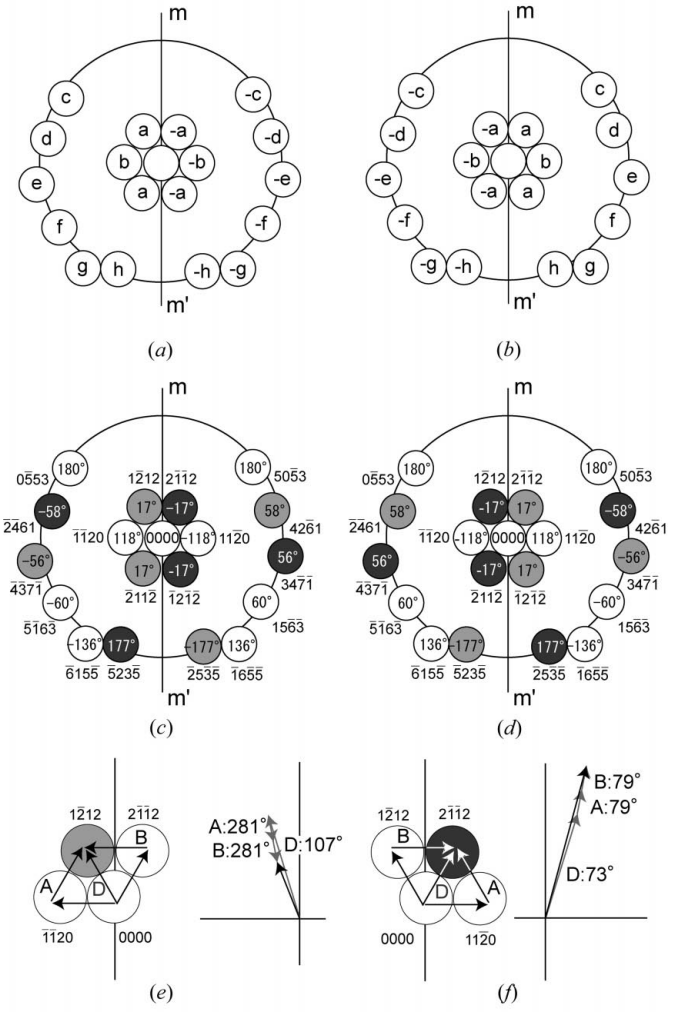

Figure 2
Schematic illustration of the appropriate zone-axis CBED patterns for (*a*) right-handed and (*b*) left-handed crystals, in which the Bijvoet pairs of reflections are observed symmetrically with respect to the symmetry line $m - m'$. The nomenclature *a*, *b*, *c*, ... indicated at the reflection disk positions schematically depict the phase angles of the corresponding reflection disks. The phase distributions for ZOLZ and FOLZ reflection disks that appear in a $[2\bar{2}0\bar{3}]$ CBED pattern of Te with the space groups $P3_121$ and $P3_221$ are shown in (*c*) and (*d*), respectively. The amplitude–phase diagrams for $(1\bar{2}12)$ and $(2\bar{1}\bar{1}2)$ ZOLZ reflection disks in the $[2\bar{2}0\bar{3}]$ CBED pattern of Te with the space group $P3_121$ are shown in (*e*) and (*f*), respectively.

3. Intensity asymmetry of Bijvoet pairs of reflections in a symmetrical zone-axis CBED pattern

3.1. Principles

As described in the previous section, nine of the 11 point groups have the appropriate zone-axis orientations in which

the Bijvoet pairs of reflections are observed symmetrically in terms of their positions, as schematically illustrated in Figs. 2(*a*) and (*b*). In the HOLZ (higher-order Laue zone) reflection disks, only FOLZ disks are depicted in Fig. 2 for simplicity. The $m - m'$ line is the symmetry line in terms of position and corresponds to the trace of the zone circle on which the appropriate zone-axis orientation is located. Many Bijvoet pairs are simultaneously observed in such a zone-axis CBED pattern, since reflections which appear symmetrically with respect to $m - m'$ are all Bijvoet pairs. In the kinematical approximation, structure factors for any *hkl* reflections are given as follows (Reimer, 1984; Williams & Carter 1996)

$$\begin{aligned} F(hkl) &= \sum_i fi(\theta)[\exp -2\pi i(hx_i + ky_i + lz_i)] \\ &= |F|exp(i\varphi), \end{aligned} \tag{3}$$

where $f_i(\theta)$ is the atomic scattering factor of the ith atom, θ is the scattering angle and (x_i, y_i, z_i) are the atomic coordinates of the ith atom. Since Bijvoet pairs are Bragg reflections which are space-group symmetry equivalents to the two members of a Friedel pair (hkl–$\overline{hkl}$), the two members of a Bijvoet pair possess identical amplitude but opposite phase, in principle, as is readily known from the following relationship

$$F(hkl) = \left|F(hkl)\right| \exp(i\varphi) \text{ and } F(\overline{hkl}) = \left|F(\overline{hkl})\right| exp(-i\varphi). \tag{4}$$

This occurs for any Bijvoet pair of reflections that are arranged symmetrically with respect to the symmetry line $m - m'$ in a zone-axis CBED pattern. Then, although the arrangement of Bijvoet pairs of reflections in the CBED pattern is symmetrical with respect to $m - m'$, the phase distribution is asymmetrical with respect to $m - m'$ for each of the two enantiomorphic crystals, as schematically illustrated in Figs. 2(*a*) and (*b*). Since the right-handed crystal can be converted to the left-handed one by changing the coordinates of the atom positions from (x, y, z) to $(-x, -y, -z)$, the following relationship which is analogous to the Bijvoet relations is obtained

$$\begin{aligned} F_R(hkl) &= \left|F_R(hkl)\right| \exp(i\varphi),\ F_R(\overline{hkl}) = \left|F_R(\overline{hkl})\right| \exp(-i\varphi) \text{ and} \\ F_L(hkl) &= \left|F_L(hkl)\right| \exp(-i\varphi),\ F_L(\overline{hkl}) = \left|F_L(\overline{hkl})\right| \exp(i\varphi). \end{aligned} \tag{5}$$

This indicates that the asymmetrical phase distribution with respect to $m - m'$ in a zone-axis CBED pattern for each of the two members of enantiomorphic crystals is reversed when the handedness is reversed. In other words, the phase distributions of these Bijvoet pairs of reflections for the two enantiomorphic crystals are asymmetric with respect to $m - m'$ and are related to each other by a mirror reflection through the symmetry line $m - m'$. As is already known from the fact that the right-handed crystal can be converted to the left-handed one by changing the coordinates of the atom positions from (x, y, z) to $(-x, -y, -z)$, the symmetry line $m - m'$ in the CBED pattern, across which many Bijvoet pairs of reflections are arranged symmetrically, is mathematically a mirror for the phase distribution of these Bijvoet pairs of reflections for enantiomorphic crystals.

In the kinematical approximation, the intensity (amplitude) distribution in the CBED pattern is still considered to be symmetrical with respect to $m - m'$ for each of the enantiomorphic crystals, since the Bijvoet pairs, each of which has an identical amplitude, are arranged symmetrically. However, it is well known that for noncentrosymmetric crystals, the breakdown of Friedel's law occurs as a result of multiple scattering among reflections in a zone-axis CBED pattern because of the dynamical nature of electron diffraction (Cowley & Moodie, 1959; Goodman & Lehmpfuhl, 1968; Cowley, 1986). This leads to the asymmetric intensity distribution in the zone-axis CBED pattern with respect to $m - m'$ for each of the two enantiomorphic crystals. Of importance to note is that since the asymmetrical phase distribution of Bijvoet pairs of reflections in a zone-axis CBED pattern for a pair of enantiomorphic crystals is reversed with respect to $m - m'$ when the handedness is reversed, the asymmetric intensity distribution in the zone-axis CBED pattern is also reversed with respect to $m - m'$ for the pair of enantiomorphic crystals. Then the chiral identification can be easily made by inspecting the asymmetric intensity distribution of the Bijvoet pairs of reflections that are arranged symmetrically with respect to $m - m'$ in a zone-axis CBED pattern for enantiomorphic crystals belonging to the nine point groups, other than 1 and 3 in Table 1.

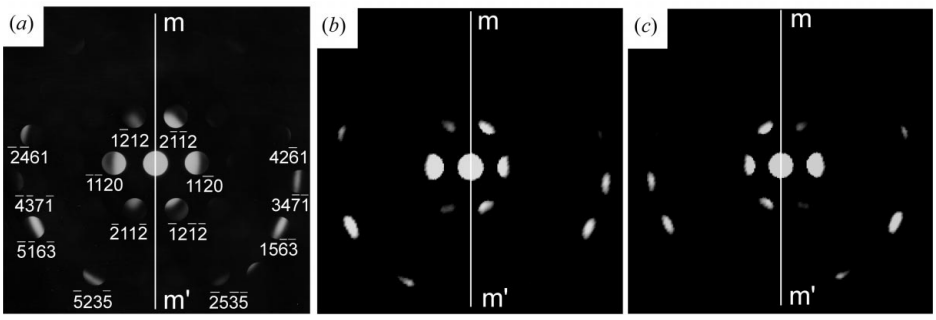

Figure 3
(*a*) Experimental and calculated $[2\bar{2}0\bar{3}]$ zone-axis CBED patterns for Te with the space groups (*b*) $P3_121$ and (*c*) $P3_221$.

3.2. Applications

We show some typical examples of chiral identification based on the above-mentioned method. Tellurium is one of the well known enantiomorphic crystals belonging to the space groups $P3_121$ and $P3_221$, as is quartz (Villars & Calvert, 1985). The point group is 321 in the hexagonal coordinate system and thus the appropriate zone-axis orientations

are of the $\langle h\bar{h}0l\rangle$-type. Here we choose $[2\bar{2}0\bar{3}]$ as an appropriate zone-axis orientation to observe Bijvoet pairs of reflections symmetrically. The phase distribution of Bijvoet pairs of reflections that appear symmetrically in a $[2\bar{2}0\bar{3}]$ CBED pattern is shown in Figs. 2(*c*) and (*d*) for Te with the space groups $P3_121$ or $P3_221$, respectively. The phase angles of the Bijvoet-pair reflections were calculated using (3). As described in §3.1, the phase distribution of both ZOLZ and HOLZ reflections is asymmetric with respect to $m - m'$ for each of the two patterns of Figs. 2(*c*) and (*d*), and is reversed with respect to $m - m'$ when the space group is changed from one to the other. Amplitude–phase diagrams for $(1\bar{2}12)$ and $(2\bar{1}\bar{1}2)$ ZOLZ reflection disks in the $[2\bar{2}0\bar{3}]$ zone-axis CBED patterns of Te with the space group $P3_121$ are shown in Figs. 2(*e*) and (*f*), respectively. In addition to the direct scattering route (*D*), multiple scattering routes (*A*) and (*B*), which are the origin of the breakdown of Friedel's law, are taken into account. Both multiple scattering routes include a partial route *via* either of two $(11\bar{2}0)$-type ZOLZ reflections. The 90° phase difference of the diffracted beam with respect to the transmitted beam is taken into account in constructing these amplitude–phase diagrams (Cowley, 1986). For the phase of the $(2\bar{1}\bar{1}2)$ ZOLZ reflection of the space group of $P3_121$, for example, the contribution from the direct route *D* is 73° (= −17 + 90°), while that from routes *A* and *B* are both 79° [= (−118 + 90) + (17 + 90°)]. When determined from the amplitude–phase diagrams, the intensity (amplitude) of the $(2\bar{1}\bar{1}2)$ ZOLZ reflection is expected to be stronger than that of the $(1\bar{2}12)$ ZOLZ reflection for the space group $P3_121$. Amplitude–phase diagrams constructed for the space group $P3_221$ indicate that the opposite is true. It is important to note that the intensities of the $(2\bar{1}\bar{1}2)$ and $(1\bar{2}12)$ ZOLZ reflections for the space group $P3_121$ are expected to be identical with those of the $(1\bar{2}12)$ and $(2\bar{1}\bar{1}2)$ ZOLZ reflections for the space group $P3_221$, respectively. In other words, the intensity distribution for these Bijvoet pairs is also asymmetric with respect to $m - m'$ for the enantiomorphic pair of crystals. For other Bijvoet pairs of reflections, the intensity asymmetry with respect to $m - m'$ is expected to occur; the stronger and weaker reflections are indicated as darker and lighter disks, respectively, in Figs. 2(*c*) and (*d*). An experimental $[2\bar{2}0\bar{3}]$ zone-axis CBED pattern of Te is shown in Fig. 3(*a*). The two CBED patterns shown in Figs. 3(*b*) and (*c*) with the same incidence as those calculated based on the space groups $P3_121$ and $P3_221$, respectively (Ishizuka, 1998). The asymmetric intensity distribution of the Bijvoet pairs of reflections for these calculated patterns is consistent with the result of the analysis of the amplitude–phase diagrams shown in Figs. 2(*c*) and (*d*), respectively, for the space groups $P3_121$ and $P3_221$. When the Bijvoet-pair intensities of the ZOLZ disks, $(1\bar{2}12)$–$(2\bar{1}\bar{1}2)$ and $(\bar{2}11\bar{2})$–$(\bar{1}2\bar{1}2)$ in the experimental pattern of Fig. 3(*a*) are compared, the intensities of the latter disks are stronger than those of the former. This indicates that Te in this case belongs to the space group $P3_121$. There are six equivalent $\langle 2\bar{2}0\bar{3}\rangle$-type directions for crystals belonging to the point group 321. All these six $\langle 2\bar{2}0\bar{3}\rangle$ incidences produce identical CBED patterns for each of the two space groups, indicating that a single CBED pattern is sufficient to identify the chirality (either $P3_121$ or $P3_221$) of Te.

The next example is $TaSi_2$ with the so-called C40 structure, which is known to have enantiomorphic crystals related to each other with respect to the reverse screw axis parallel to the hexagonal *c* axis (Villars & Calvert, 1985). The space groups of $TaSi_2$ are $P6_222$ and $P6_422$, respectively. Since the point group is 622, the appropriate zone-axis orientations are of the $\langle h\bar{h}0l\rangle$-, $\langle hh\bar{2}hl\rangle$- and $\langle hki0\rangle$-types (Table 1). Here, we choose $[3\bar{3}01]$ as an appropriate zone-axis orientation. The phase distributions of the Bijvoet pairs of reflections that appear in a $[3\bar{3}01]$ CBED pattern are shown in Figs. 4(*a*) and (*b*) for $TaSi_2$ with the space groups $P6_222$ and $P6_422$, respectively. In this case, the phase distribution of HOLZ reflections is asymmetric with respect to $m - m'$ for each of the two patterns in Figs. 4(*a*) and (*b*), and is reversed with respect to $m - m'$ when the space group is changed from one to the other. Strictly

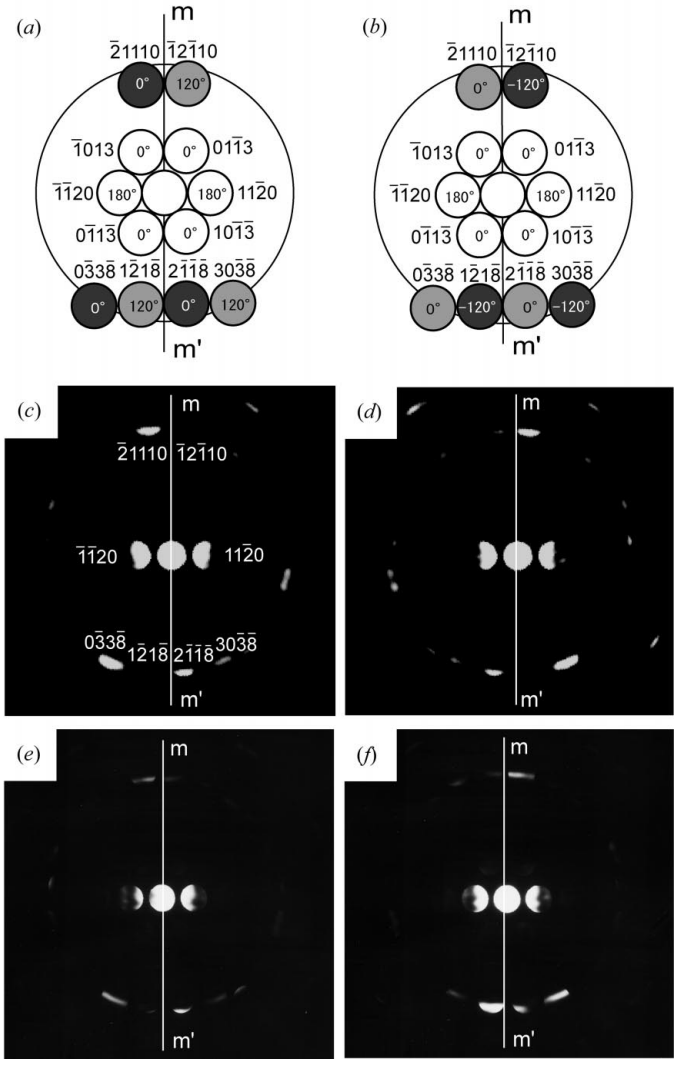

Figure 4
Phase distribution for ZOLZ and FOLZ reflection disks that appear in a $[3\bar{3}01]$ zone-axis CBED pattern of $TaSi_2$ with the space groups (*a*) $P6_222$ and (*b*) $P6_422$. The corresponding calculated and experimental CBED patterns are shown in (*c*) and (*f*) for $P6_222$ and in (*d*) and (*f*) for $P6_422$.

speaking, the relative values of the phase angles of the Bijvoet pairs of reflections as opposed to their absolute values are reversed when the space group is changed. For example, the phase angle of the $(2\bar{1}\bar{1}\bar{8})$ reflection is delayed by 120° with respect to that of the $(1\bar{2}1\bar{8})$ reflection for the space group $P6_222$ (Fig. 4*a*), while the phase angle of the $(1\bar{2}1\bar{8})$ reflection is delayed by 120° with respect to that of the $(2\bar{1}\bar{1}\bar{8})$ reflection for the space group $P6_422$ (Fig. 4*b*). On the other hand, the phase distribution of the ZOLZ reflections is symmetric with respect to $m - m'$ and identical for both the two patterns. This is because of the fact that the l index for all ZOLZ reflections in the $[3\bar{3}01]$ CBED pattern is $l = 3n$ (n: integer), which does not produce different phase angles for Bijvoet pairs of reflections (Hahn, 1996). The asymmetric phase distribution also appears for ZOLZ reflections when the zone-axis orientation is chosen so that the ZOLZ reflections with the l index $l \neq 3n$ appear. This can be realised when the zone-axis orientation is, for example, $[2\bar{2}01]$ and $[1\bar{1}01]$. In these cases, the chiral identification can be made by noting the intensity asymmetry in Bijvoet pairs of ZOLZ reflections, as in the case of Te (Figs. 2 and 3). In the case of the $[3\bar{3}01]$ CBED patterns of $TaSi_2$, however, the intensity asymmetry in Bijvoet pairs of FOLZ reflections is used for the chiral identification. The construction of the amplitude–phase diagrams for $(1\bar{2}1\bar{8})$ and $(2\bar{1}\bar{1}\bar{8})$ FOLZ reflection disks in the $[3\bar{3}01]$ zone-axis CBED pattern, taking into account the multiple scattering routes *via* each of two $(11\bar{2}0)$-type ZOLZ reflections, indicates that the intensity (amplitude) of the $(2\bar{1}\bar{1}\bar{8})$ FOLZ reflection is expected to be stronger than that of the $(1\bar{2}1\bar{8})$ FOLZ reflection for the space group $P6_222$, while the opposite is true for the space group $P6_422$. The intensity distribution of the FOLZ reflection disks in this case is expected to be reversed with respect to $m - m'$ when the space group changes from one to the other. The stronger and weaker Bijvoet pairs of FOLZ reflections expected from the consideration based on amplitude–phase diagrams are indicated as darker and lighter disks, respectively, in Figs. 4(*a*) and (*b*). When the intensity for Bijvoet pairs of FOLZ disks, for example, $(0\bar{3}\bar{3}\bar{8})$–$(30\bar{3}\bar{8})$, $(2\bar{1}\bar{1}\bar{8})$–$(1\bar{2}1\bar{8})$ and $(\bar{2},1,1,10)$–$(\bar{1},2,\bar{1},10)$ are compared, the intensities of the former disks are expected to be stronger than those of the latter disks in Fig. 4(*a*), while the opposite is true in Fig. 4(*b*). The expected intensity distribution for the Bijvoet

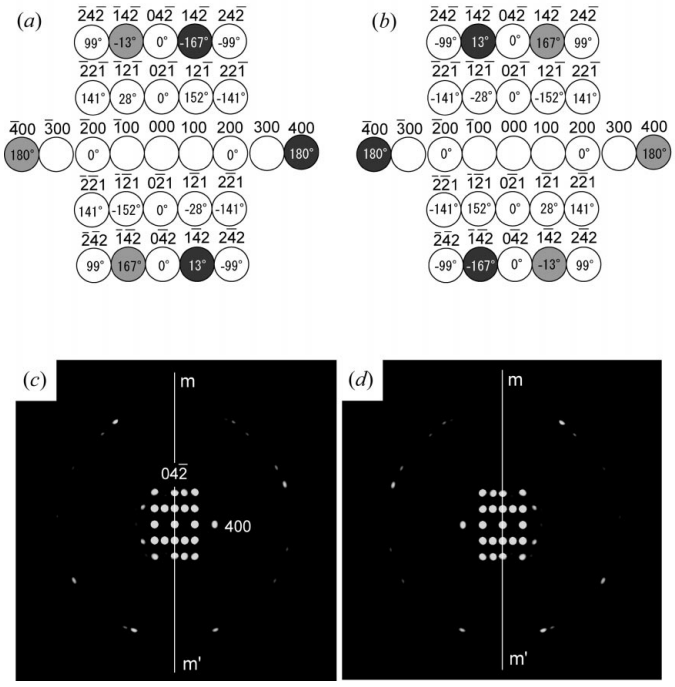

Figure 5
Phase distribution for ZOLZ reflection disks that appear in a [012] zone-axis CBED pattern of (*a*) L- and (*b*) D-α glutamic acid. The corresponding calculated CBED patterns are shown in (*c*) for L- and in (*d*) for D-α glutamic acid.

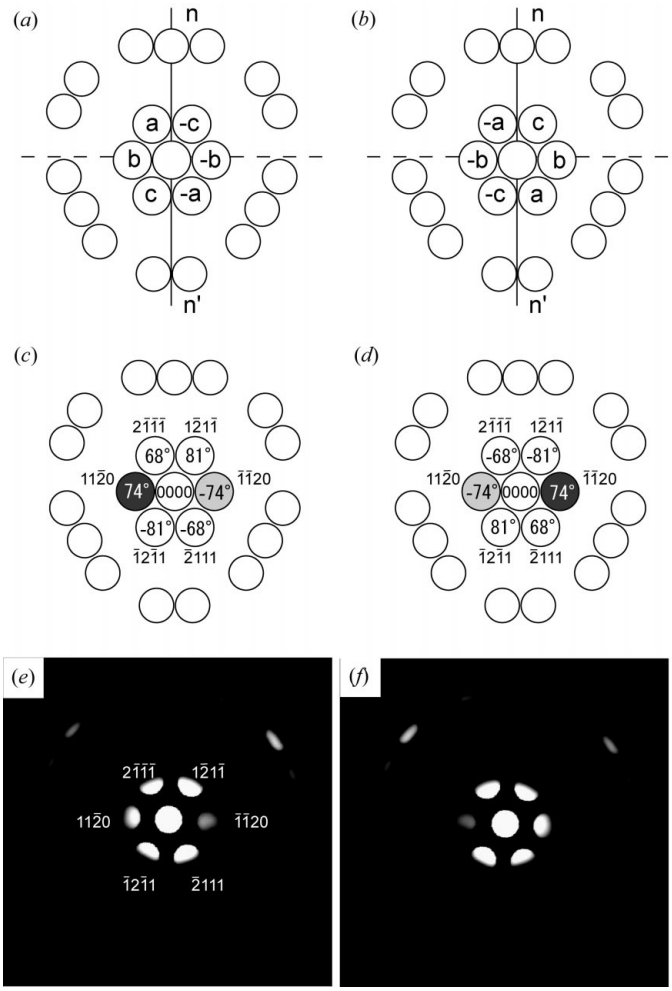

Figure 6
(*a*) and (*b*) Schematic illustration of the zone-axis CBED patterns of enantiomorphic crystals belonging to the point groups of 1 and 3, in which all $\pm g$ reflection pairs of ZOLZ disks are Bijvoet pairs. The nomenclatures *a*, *b*, *c*,... indicated at reflection disk positions schematically depict the phase angles of the corresponding reflection disks. The phase distributions for ZOLZ reflection disks that appear in a $[1\bar{1}03]$ CBED pattern of B_2O_3 with the space groups $P3_1$ and $P3_2$ are shown in (*c*) and (*d*), respectively. The corresponding calculated CBED patterns are shown in (*e*) and (*f*) for the space groups $P3_1$ and $P3_2$, respectively.

pairs of reflections shown in Figs. 4(*a*) and (*b*), respectively, for the space groups $P6_222$ and $P6_422$ is well reproduced in the calculated [$3\bar{3}01$] zone-axis CBED patterns of $TaSi_2$ for both the space groups (Figs. 4*c* and *d*). $TaSi_2$ with both the space groups can be obtained as a thin film for the racemic twins (Inui *et al.*, 2003). The asymmetric intensity distribution of the reflection disks in the experimental [$3\bar{3}01$] zone-axis CBED patterns of $TaSi_2$ with the space groups $P6_222$ and $P6_422$ (Figs. 4*e* and *f*, respectively) coincides well with that calculated based on the space groups $P6_222$ and $P6_422$ (Figs. 4*c* and *d*, respectively). Thus, there is no intensity asymmetry in the ZOLZ reflections. The intensity asymmetry in FOLZ reflections with respect to $m - m'$ can be utilized for chiral identification. There are 12 equivalent $\langle 3\bar{3}01\rangle$-type directions for crystals belonging to the point group 622. Only a single CBED pattern is sufficient to identify the chirality (either $P6_222$ or $P6_422$) of $TaSi_2$, since all 12 equivalent $\langle 3\bar{3}01\rangle$ incidences produce the identical CBED patterns for each of the two space groups.

The last example for chiral identification is α-glutamic acid, which is one of the organic amino acid crystals. α-Glutamic acid possesses an asymmetric (chiral) C atom and the glutamic acid molecules can be either left-handed or right-handed within the space group of $P2_12_12_1$, depending on how the surrounding substitutional groups attach to the C atom (Hirayama *et al.*, 1980). These crystals are known as L- and D-α-glutamic acid, respectively. Since the point group is 222, the appropriate zone-axis orientations are of the $\langle hk0\rangle$-, $\langle 0kl\rangle$- and $\langle h0l\rangle$-types (Table 1). We choose [012] as an appropriate zone-axis orientation. The phase distributions for the Bijvoet pairs of ZOLZ reflections are illustrated in Figs. 5(*a*) and (*b*) for L- and D-α-glutamic acid, respectively. Although the phase distributions for FOLZ reflections are not shown in the figures for simplicity, the phase distributions of both ZOLZ and HOLZ reflections are asymmetric with respect to $m - m'$ for each of the two patterns shown in Figs. 5(*a*) and (*b*), and are reversed with respect to $m - m'$ when the handedness is reversed. Owing to the asymmetric phase distribution of the Bijvoet pairs of ZOLZ and FOLZ reflections, their asymmetric intensity distribution with respect to $m - m'$ is clearly observed in each of the corresponding calculated images in Figs. 5(*c*) and (*d*). The asymmetric intensity distribution is obviously reversed with respect to $m - m'$ when the handedness is reversed. The chiral identification can thus be easily made by noting the asymmetric intensity distribution of these Bijvoet pairs of reflections.

4. Intensity asymmetry of Bijvoet pairs of reflections for the point groups 1 and 3

Bijvoet pairs of reflections that appear in ZOLZ as $\pm\mathbf{g}$ reflections are utilized for the chiral identification of enantiomorphic crystals belonging to the point groups 1 and 3. Since all $\pm\mathbf{g}$ reflection pairs of ZOLZ disks are Bijvoet pairs, the phase distribution of ZOLZ disks in any zone-axis CBED pattern is asymmetric, as schematically illustrated in Figs. 6(*a*) and (*b*) for a pair of enantiomorphic crystals belonging to these two point groups. Although FOLZ reflection disks appear symmetrically with respect to $n - n'$ when the zone-axis orientation is on a low-indexed zone circle corresponding to $n - n'$, none of them are Bijvoet pairs. From the Bijvoet relations [see (2)] it can be easily seen that the phase distribution of the ZOLZ reflections for one of the two enantiomorphic crystals is related to that of the other by a 180° rotation about the incident beam direction. Once the breakdown of Friedel's law occurs as a result of multiple scattering among these ZOLZ reflections, the intensity distribution for each of the two CBED patterns shown in Figs. 6(*a*) and (*b*) loses its centrosymmetry with respect to the transmitted (center) disk. The intensity distribution of one of the enantiomorphic pair is therefore related to that of the other by a 180° rotation about the incident beam direction, as with the phase distribution. Of importance to note is that in general, FOLZ reflections distribute asymmetrically with respect to a line (indicated with - - - in the figures) that is perpendicular to $n - n'$ and passes through the center disk. Then, a 180° rotation of the intensity distribution of ZOLZ reflections can be readily known when referring to the asymmetric distribution (location) of FOLZ reflections in a zone-axis CBED pattern. The chiral identification can thus be made easily by inspecting the asymmetric intensity distribution of these Bijvoet pairs of ZOLZ reflections in such a zone-axis CBED pattern.

We now show an example of chiral identification based on the above-mentioned method using B_2O_3 (point group 3, space groups $P3_1$ and $P3_2$; Villars & Calvert, 1985). As described in §2, there is no specification for appropriate zone-axis orientations. In other words, we need to choose an appropriate zone-axis orientation (in which the above-mentioned intensity asymmetry is significant) from the phase angle calculation or computer simulation of CBED patterns for various zone-axis orientations. We choose [$1\bar{1}03$] as the zone-axis orientation for the chiral identification of B_2O_3. The phase distribution of ZOLZ reflections in the [$1\bar{1}03$] CBED pattern is shown in Figs. 6(*c*) and (*d*) for B_2O_3 with the space groups $P3_1$ and $P3_2$, respectively. The phase distribution of ZOLZ reflections in the [$1\bar{1}03$] CBED pattern of one of the two space groups is related to that of the other by a 180° rotation about the incident beam direction. The construction of amplitude–phase diagrams for ($11\bar{2}0$) and ($\bar{1}\bar{1}20$) ZOLZ reflection disks in the [$1\bar{1}03$] zone-axis CBED patterns indicates that the intensity of the former reflection is stronger than that of the latter for the space group $P3_1$, while the opposite is true for the space group $P3_2$. The expected intensity distribution in the [$1\bar{1}03$] CBED patterns for both the space groups of $P3_1$ and $P3_2$ is well reproduced in those calculated based on the space groups $P3_1$ and $P3_2$, respectively (Figs. 6*e* and *f*). Owing to the asymmetric phase distribution of Bijvoet pairs of ZOLZ reflections, their asymmetric intensity distribution is clearly observed in each of these CBED patterns. The asymmetric intensity distributions for the two space groups are obviously related to each other by a 180° rotation about the incident beam direction. The chiral identification can easily be made by noting the asymmetric intensity distribution of these Bijvoet pairs of reflections.

5. Discussion

Characteristics of the present method are summarized as follows.

(i) All the possible pairs of enantiomorphic crystals that are allowed to exist in crystallography can be uniquely determined by taking a single symmetrical zone-axis CBED pattern in the TEM.

(ii) Information on possible space group(s) and atomic coordinates (position parameters) for the enantiomorphic crystal of interest is needed for chiral identification, since the phase angle and distribution vary according to these parameters.

(iii) A conventional TEM is sufficient as long as a CBED technique is available. No special and costly design feature such as a field-emission gun is needed for the TEM.

(iv) Unlike in X-ray diffraction, the present TEM method does not require a high power source such as synchrotron radiation, special techniques such as the MIR method, or particular target materials to enhance anomalous scattering.

(v) Once the specimen is tilted to an appropriate zone-axis orientation, the exposure time for a CBED pattern is usually of the order of a second or less, which is less time by far than that needed for acquiring intensity peaks for various Bijvoet pairs of reflections by X-ray diffraction.

(vi) On top of this, the analysis of asymmetry in the intensity of reflection disks of Bijvoet pairs in the present method is so straightforward that the time needed for analysis is also shorter by far than that usually needed for intensity analysis in X-ray diffraction. If the relevant CBED patterns are computer-calculated beforehand, the chiral identification is readily made at the time of the actual observation in a 'fingerprinting' way and does not require any further analysis and calculation.

(vii) Since the present method is based on a comparison of the intensity asymmetry between Bijvoet pairs of reflections, a thin crystal is desirable. The maximum crystal thickness is limited by the extinction distance of reflections relevant to multiple scattering, which is usually of the order of a few tens of nanometers (Reimer, 1984; Cowley, 1986; Williams & Carter 1996). Chiral identification may also be made for thicker crystals by noting the difference (asymmetry) in the extinction pattern appearing within the disks of these Bijvoet pairs of reflections (Vermaut *et al.*, 1997; Cherns *et al.*, 1998; Hong *et al.*, 2002). The asymmetric pattern within the disks of these Bijvoet pairs is also from the asymmetric phase distribution. However, in this case extensive computer simulation of the CBED patterns is needed for chiral identification, since the extinction patterns that appear within the disks of these reflections of the Bijvoet pairs for thicker crystals vary with the crystal thickness rather sensitively (Vermaut *et al.*, 1997; Cherns *et al.*, 1998; Hong *et al.*, 2002).

(viii) As the present method is based on electron diffraction in the TEM, where an electron probe of nanometer size is easily obtained (the probe size used in the present study is typically a few tens of nanometers in diameter), even a tiny crystal containing numerous crystal lattice defects can be used for chiral identification, unlike in X-ray diffraction where large-sized single crystals of high quality are usually used. Since a nanometer-sized probe is usually available in the TEM, the present method can be utilized not only for bulk materials, but also for nanometer-structured complex materials.

(ix) Added to this, the significant scattering capability of electrons for light elements gives rise to the advantage of applying the present method to organic crystals without any special sample preparation techniques such as the MRI method.

The present method is of importance since this provides the first electron diffraction method for chiral identification of all enantiomorphic crystals that are allowed to exist in crystallography. In contrast to this, the electron diffraction methods so far proposed for chiral identification (Goodman & Secomb, 1977; Goodman & Johnson, 1977; Tanaka *et al.*, 1985) cannot be easily extended to all possible enantiomorphic crystals, since all the methods involve a rather complicated calculation of the dynamical electron diffraction for particular reflections. The method proposed by Goodman & Secomb (1977) is similar to the present method in that the intensities of particular reflections are interpreted in terms of the total number of phases for relevant reflections, but is different from the present method in that at least two CBED patterns with different incident beam directions are needed for chiral identification. The major difficulty of the method by Goodman & Secomb (1977) is that they did not describe how the zone-axis orientation and the reflections to be inspected were chosen for a particular enantiomorphic crystal, *i.e.* quartz. The method proposed for MnSi by Tanaka *et al.* (1985) utilizes the asymmetry of the extinction patterns appearing within the reflection disks of opposite sign (*i.e.* Friedel pairs). This is exactly what is discussed for thick crystals in (vii) as the characteristics of the present method. However, Tanaka *et al.* (1985) did not describe the origin of the asymmetry of the extinction patterns appearing within the reflection disks of opposite sign and how the method can be extended to other enantiomorphic crystals. Recently, a new coherent CBED method has been proposed, in which chiral identification is made by noting the difference in interference fringe patterns that appear in the overlapping regions between reflection disks, depending on whether the nanometer-sized probe position is on twofold axes or twofold screw axes in the projection of the unit cell (Tsuda *et al.*, 2000; Saitoh *et al.*, 2001). This method allows the theoretical chiral identification of crystals containing twofold axes perpendicular to the principle axes, but the practice is terribly difficult because of the requirements for the very high stability of the electron microscope, in particular the problem of specimen drift.

If each one of the enantiomorphic pair exists separately, their physical and chemical properties are identical (Mason, 1982; Crossley, 1995; Brown, 1997), and therefore chiral identification is only of scientific importance, in particular, for inorganic crystals. However, we believe that this method may uncover fruitful applications in the investigation of organic crystals which exhibit optical bioactivities. These involve

organic biomaterials related to pharmaceuticals, proteins, food *etc*. Although organic crystals have been known to be easily damaged by electron beam illumination, the cooling of organic specimens down to liquid-He temperature has been recently reported to be very effective in reducing the electron illumination damage (Fujiyoshi *et al.*, 1991).

6. Conclusions

A new CBED method is proposed for the chiral identification of enantiomorphic crystals, in which the asymmetry in the intensity of the reflections of the Bijvoet pairs in an experimental symmetrical zone-axis CBED pattern is compared with that of a computer-simulated CBED pattern. While the intensity (amplitude) distribution in the CBED pattern is considered to be symmetrical in the kinematical approximation, the intensity asymmetry that occurs for the reflections of these Bijvoet pairs results from multiple scattering (dynamical nature of electron diffraction) among the relevant Bijvoet pairs of reflections, each pair of which has identical amplitudes and different phase angles. Therefore, the crystal thickness where chiral identification is made with the present method is limited by the extinction distance of Bijvoet pairs of reflections relevant to multiple scattering to produce the intensity asymmetry, which is usually of the order of a few tens of nanometers. This situation can be achieved by choosing the appropriate zone-axis orientations for all the possible enantiomorphic crystals. With the present method, a single CBED pattern is sufficient and chiral identification can be made for all the possible enantiomorphic crystals.

This work was supported by a Grant-in-Aid for Scientific Research from the Ministry of Education, Science and Culture (No. 14350369) and in part by the Mitsubishi Foundation.

References

Bijvoet, J. M., Peerdeman, A. F. & van Bommel, A. J. (1951). *Nature*, **168**, 271–272.
Brown, C. (1997). *Chirality in Drug Design and Synthesis.* New York: Academic Press.
Burns, G. & Glazer, A. M. (1990). *Space Groups for Solid State Scientists*, 2nd ed. Boston: Academic Press.
Cherns, D., Young, W. T., Saunders, M., Steeds, J. W., Ponce, F. A. & Nakamura, S. (1998). *Philos. Mag. A*, **77**, 273–286.
Cowley, J. M. (1986). *Diffraction Physics.* Amsterdam: North-Holland.
Cowley, J. M. & Moodie, A. F. (1959). *Acta Cryst.* **12**, 360–367.
Crossley, R. (1995). *Chirality and Biological Activity of Drugs.* London: CRC.
Drenth, J. (1994). *Principles of Protein X-ray Crystallography*. Berlin: Springer-Verlag.
Fujiyoshi, Y., Mizusaki, T., Morikawa, K., Yamagishi, H., Aoki, Y., Kihara, H. & Hrada, Y. (1991). *Ultramicroscopy*, **38**, 241–251.
Glusker, J. P., Lewis, M. & Rossi, M. (1994). *Crystal Structure Analysis for Chemists and Biologists.* New York: VCH.
Glusker, J. P. & Trueblood, K. N. (1972). *Crystal Structure Analysis: A Primer.* New York: Oxford University Press.
Goodman, P. & Johnson, A. W. S. (1977). *Acta Cryst.* A**33**, 997–1001.
Goodman, P. & Lehmpfuhl, G. (1968). *Acta Cryst.* A**24**, 339–347.
Goodman, P. & Secomb, T. W. (1977). *Acta Cryst.* A**33**, 126–133.
Hahn, T. (1996). *International Tables for Crystallography, Volume A: Space-Group Symmetry*, 4th revised ed., pp. 786–792. Dordrecht: Kluwer Academic Press.
Hirayama, N., Shirahata, K., Ohashi, Y. & Sasada, Y. (1980). *Bull. Chem. Soc. Jpn*, **53**, 30–35.
Hong, S.-K., Hanada, T., Ko, H.-J., Chen, Y. F., Yao, T., Imai, D., Araki, K., Shinohara, M., Saitoh, K. & Terauchi. M. (2002). *Phys. Rev. B*, **65**, 115331-1-10.
Inui, H., Fujii, A., Hashimoto, T., Tanaka, K., Yamaguchi, M. & Ishizuka, K. (2003). *Acta Mater.* **51**, 2285–2296.
Ishizuka, K. (1998). *Proc. Int. Symp. on Hybrid Analyses for Functional Nanostructure*, edited by M. Shiojiri & N. Nishio, pp. 69–74. Tokyo: Japanese Society of Electron Microscopy.
James, R. W. (1982). *The Optical Principles of the Diffraction of X-rays.* Woodbridge: Ox Bow Press.
Mason, S. F. (1982). *Molecular Optical Activity and the Chiral Discriminations.* Cambridge University Press.
McPherson, A. (1982). *Preparation and Analysis of Protein Crystals.* New York: John Wiley and Sons.
Mead, C. A. (1974). *Symmetry and Chirality.* Berlin: Springer-Verlag.
Ramaseshan, S. (1964). *Advanced Methods of Crystallography*, edited by G. N. Ramachandran, pp. 67–95. London: Academic Press.
Reimer, L. (1984). *Transmission Electron Microscopy*. Berlin: Springer-Verlag.
Saitoh, K., Tsuda, K., Terauchi, M., Tanaka, M. & Goodman, P. (2001). *Acta Cryst.* A**57**, 219–230.
Spence, J. C. H. & Zuo, J. M. (1992). *Electron Microdiffraction.* New York: Plenum Press.
Srinivasan, R. (1972). *Advances in Structure Research by Diffraction Methods*, edited by W. Hoppe & R. Mason, pp. 103–197. New York: Interscience.
Stout, G. H. & Jensen, L. H. (1989). *X-ray Structure Determination: A Practical Guide*, 2nd ed. New York: John Wiley and Sons.
Tanaka, M., Takayoshi, H., Ishida, M. & Endoh, Y. (1985). *J. Phys. Soc. Jpn*, **54**, 2970–2974.
Tanaka, M. & Terauchi, M. (1985). *Convergent-Beam Electron Diffraction.* Tokyo: Jeol-Maruzen.
Tsuda, K., Saitoh, K., Terauchi, M., Tanaka, M. & Goodman, P. (2000). *Acta Cryst.* A**56**, 359–369.
Vermaut, P., Ruterana, P. & Nouet, G. (1997). *Philos. Mag. A*, **76**, 1215–1234.
Villars, P. & Calvert, L. D. (1985). *Pearson's Handbook of Crystallographic Data for Intermetallic Phases.* Metals Park: American Society for Metals.
Williams, D. B. & Carter, C. B. (1996). *Transmission Electron Microscopy.* New York: Plenum Press.